



Project acronym: GROUND-MED

Project title: Advanced ground source heat pump systems for heating and cooling in Mediterranean climate

Start date of project: 1 January 2009

Duration: 60 months

Deliverable D4.1: Generalised Dynamic Control Model

Version: 1st

Due date of deliverable: 31 October 2009

Actual submission date: 1 March 2010

Organisation name of lead contractor for this deliverable:

University College Dublin

Project co-funded by the European Commission within FP7 Programme		
Dissemination level		
PU	Public	X
PP	Restricted to other programme participants (including the Commission Services)	
RE	Restricted to a group specified by the Consortium (including the Commission Services)	
CO	Confidential, only for members of the consortium (including the Commission Services)	

GROUND-MED WP4 Integrated System Control

DELIVERABLE D4.1

Generalised Dynamic Control Model

Authors

Donal Finn and Kilian Edwards (UCD)

Contributors

Jose Miguel Corberan and Carla Montagud (UPV)

Bjorn Palm (KTH)

Henk Witte (GroenHolland)

Anibal de Almeida (ISR)



**School of Electrical, Electronic & Mechanical Engineering
University College Dublin (UCD)**

Contents

Nomenclature.....	iv
1. Introduction.....	1
2. Background and context: control strategies.....	2
2.1 Heat pump capacity control	
2.2 Secondary side fluid control.....	
2.3 Temperature setback and bandwidth control	
2.4 Previous simulation models	
3. Methodology.....	8
3.1 Description of the scope of a potential physical system	
3.2 Performance characterisation of heat pump system	
3.2.1 Heat pump model	
3.2.2 Circulation pumps	
3.2.3 Fan coil	
3.2.4 Water storage tank	
3.2.5 Hydronic pipe network	
3.3 Building model characterisation	
3.4 Ground model characterisation	
4. Simulation description.....	15
4.1 Heat pump model	
4.2 Circulation pumps	
4.3 Fan coil	
4.4 Water storage tank	
4.5 Hydronic Pipe network	
4.6 Building model	
4.7 Execution of EES simulation	
4.8 Initialising System Variables	
4.9 Execution of EES simulation	
5. Simulation results.....	25
5.1 Steady state performance	
5.2 Quasi-steady state performance	
6. Conclusions.....	35
References.....	36

Nomenclature

A	Heat transfer surface area (m^2)
C_p	Specific heat capacity at constant pressure ($J.kg^{-1}K^{-1}$)
F_{REQ}	Circulation pump frequency (Hz)
\dot{m}	Mass flow rate ($kg.s^{-1}$)
M	Mass (kg)
P	Perimeter (m)
\dot{P}_{HP}	Heat pump compressor power (W)
\dot{P}_{SYSTEM}	System power (heat pump, fan coils, internal pump, external pump) (W)
\dot{Q}	Heat transfer rate (W)
\dot{Q}_c	Cooling thermal load (W)
$\dot{Q}_{condenser}$	Condenser thermal load (W)
$\dot{Q}_{evaporator}$	Evaporator thermal load (W)
T	Temperature (C)
T_{RCI}	Water return temperature for the building circuit (K)
T_{RCE}	Water return temperature for the external circuit (K)
t	Time (s)
U	Overall heat transfer coefficient ($W.m^{-2}K^{-1}$)
v	Velocity ($m.s^{-1}$)
V_{CI}	Water mass flow rate in the internal circuit ($kg.s^{-1}$)
V_{CE}	Water mass flow rate in the external circuit ($kg.s^{-1}$)
\dot{V}	Volumetric flow rate ($m^3.s^{-1}$)
Δt	Time step
Δx	Distance between two consecutive nodes

Greek symbols

ϵ	Heat exchanger effectiveness
ρ	Density ($kg.m^{-3}$)

Subscripts

FC	Fan coil
HP	Heat pump
ICP	Internal circulation pump
i	Inlet
o	Outlet

List of Figures

- Figure 3.1 Generalised Heat Pump System
- Figure 3.2 Compressor power consumption (IMST-ART) and correlated fit.
- Figure 3.3 Circulation Pump Performance Correlation
- Figure 3.4 Fan Coil UA Correlation.
- Figure 4.1 Conceptual Model Architecture
- Figure 4.1 Conceptual Model Architecture
- Figure 5.1 Heating capacity and cooling capacity vs. circulation pump frequencies.
- Figure 5.2 System COP vs circulation pump frequencies (heating mode).
- Figure 5.3 Daily profile of supply, return and space temperature (cooling mode).
- Figure 5.4 Building water return temperature evolution
- Figure 5.5 Set-point control of space temperature
- Figure 5.6 Building return temperature as a function of return water bandwidth
- Figure 5.7 Energy consumption and SPF predictions

List of Tables

- Table 4.1 EES code for heat pump in cooling mode
- Table 4.2 EES code for heat pump in heating mode
- Table 4.3 Heat pump boundary conditions and water properties
- Table 4.4 Model of indoor hydronic circuit circulation pump in EES
- Table 4.5 Model of outdoor ground loop circulation pump in EES
- Table 4.6 Water and Air heat transfer properties
- Table 4.7 Calculation of NTU and effectiveness of fan coil units
- Table 4.8 Calculation of water/air temperature and energies across fan coil units
- Table 4.8 Calculation of water/air temperature and energies across fan coil units
- Table 4.8 Calculation of water/air temperature and energies across fan coil units
- Table 4.11 Mathematical description of temperature evolution of water travelling
- Table 4.12 Mathematical description of temperature evolution of water
- Table 4.13 Model of energy balance in the conditioned space
- Table 4.14 Initial variable values for EES model
- Table 4.15 Check stop function governing simulation duration
- Table 4.16 Definition of the simulation time-step and convergence criteria in EES
- Table 5.1 System performance parameters as a function of return water bandwidth
- Table 5.2 System performance parameters as a function of return water bandwidth

1. INTRODUCTION

This report constitutes Deliverable 4.1 entitled *Generalised Dynamic Control Model* as part of Work Package 4 (WP4) of the GROUNDMED project. The deliverable was completed in collaboration with partners UPV (Universidad Politecnica de Valencia), KTH (Royal Institute of Technology) and GroenHolland. The overall aim of Deliverable 4.1 is to develop a generalised mathematical model of a building integrated heat pump system that can be used for simulating and evaluating different control strategies, as per the GROUNDMED programme. Moreover, it is intended that the model should have the capability of capturing system dynamics while avoiding unnecessary system complexity. Specifically the model should allow for estimation of heating/cooling capacity and electrical power consumption of the overall heat pump system on the basis of the following variables: building and ground loop return temperatures, building and ground loop water massflow rates, chiller/heater unit air massflow rates and heat pump compressor speed. The report is divided into a number of sections as follows. Section 2 reviews various control strategies deployed for heat pump systems and summarises different mathematical modelling approaches used to model heat pump and similar systems. Section 3 describes the methodology used to develop the mathematical model developed in this work. In Section 4, the simulation model code is summarised and explained. Section 5 illustrates the capabilities of the model for analysis of steady state performance, quasi-steady state conditions and accumulated performance criteria. Section 6 concludes the report.

2. BACKGROUND

Recent developments in global energy perspectives have resulted in an increased interest in the deployment of ground source heat pumps (GSHP) (Yang et al, 2009). One issue that is increasingly gaining interest is the question of improved system integration and optimisation by the utilisation of improved control algorithms. Increased performance of heat pumps can be attributed to advances in component design and efficiencies as well as the deployment of sophisticated control strategies (Yang and Pedersen, 2007).

A variety of control strategies can be deployed in heat pump systems such as compressor capacity control, throttle control utilising electronic expansion valves, secondary fluid flow control and control of temperature set-points and bandwidths. Using more advanced control strategies and technology can aid in reducing both systems oscillations and the design load of the heat pump while increasing efficiency (Sakellari et al, 2006).

In developing the mathematical model described in this deliverable, the types of control strategies that may be applied to a system were considered. It was also required that the model should be sufficiently generalised and adaptable, so that a variety of control strategies and systems can be analysed. Some possible control strategies for a ground source heat pump include control of the room temperature set-point and bandwidth, heat pump capacity, secondary fluid flow-rate, fan speeds, as well as the use of passive or active thermal energy storage.

2.1. Heat pump capacity control

The most common type of capacity control currently deployed in commercial ground source heat pumps appears to be on/off cycling of compressor units, either with or without energy storage (Flach-Malaspina et al 2004). When operating at part load control is achieved through on/off cycling of the compressor and supplemental heating is activated when demand exceeds the heat pump capacity (Karlsson and Fahlen 2003). On/off control operates effectively at design load conditions, but under part load conditions inefficiencies can increase due to compressor cycling. These cycling inefficiencies were investigated by Krause and Bullard (1994) and Wang and

Lavan (1999) and can be attributed to refrigerant migration and cooling down during the off period of a compressor cycle. The inefficiencies associated with on/off control at part load can be somewhat reduced using more advanced control strategies such as prognostic control, which predicts future heat loads (Sakellari *et al*, 2006). In this particular study the solar temperature was monitored and the compressor was set to off before the temperature had reached about one third of its maximum predicted level. The use of variable speed compressors by means of inverter control has attracted considerable research interest and recent evidence indicates their gradual adaption by certain heat pump manufacturers (Shao *et al* 2004). Through the use of variable speed compressors, coupled with the deployment of an electronic expansion device (EEV), the modulation range of the capacity can be varied from 20-130% of a typical compressor nominal load (Chen *et al* 2004). Simulation models comparing the performances of on/off and variable speed control at part load have been developed by Yang and Pedersen (2007) and Qureshi and Tassou (1995). They demonstrate the potential saving available through implementation of variable speed compressor control at part load. However, these studies appear to exclude the inherent inefficiencies associated with variable speed compressors due to the idealised simulation models used. Cuevas and Lebrun (2009) and Shao *et al* (2004) demonstrated the inefficiencies associated with the inverter in variable speed compressors, showing a substantial degradation of performance when the compressor is operated outside its designed frequency range (usually between 35 and 70Hz).

Karlsson and Fahlen (2003) evaluated on/off and variable speed compressor control. They noted that the main benefit of using a variable speed compressor was a reduction in the need for supplementary heating. However, the savings expected from the variable speed compressor were less than expected because of losses attributed to reduced electrical motor efficiency at lower speeds. Frequency converter and compressor heat losses also contributed to lower variable speed test results than predicted in theory. In a later study, Karlsson and Fahlen (2007) tested a heat pump designed for variable speed. The efficiency increased by 4-11% when operating at part load while the previous modified variable speed heat pump showed an efficiency drop of 4%. Savings due to the use of variable speed compressors were also reported in other earlier studies by Shimma *et al* (1988), Vargas and Parise (1994) and Aprea *et al* (2004).

Many modern central cooling plants are designed so that a combination of variable and constant speed compressors are utilised, rather than relying exclusively on variable speed systems (Yu and Chan 2008). Jain and Bullard (2004) evaluated, using a simulation model, the benefits of using a variable speed and a number of single speed compressors in air conditioning systems. Ma and Wang (2009) designed a centralised cooling system for a large high-rise building. Multiple single speed compressors were used in cooling system along with heat exchanger and variable speed pumps in each section. The use of multiple compressors was shown to reduce energy consumption in both systems.

2.2. Secondary side fluid control

Overall (system) heat pump COP is dependent on the power consumed by both parasitic elements, such as pumps and fan coils, as well as the compressor. Therefore it is of interest to reduce this energy usage where possible. Control of the secondary fluid can aid with reducing energy usage and improving system performance (Fahlén and Karlsson, 2005). Very few studies deal the subject of secondary side fluid control in ground source heat pumps when compared to air-air heat pump systems. Chen et al (2004) studied air flowrate and variable speed compressor control to aid with set-point control in an air-to-air chiller. However, as mentioned in a study by Riviere (2004), the thermal dynamics of water, when used as a secondary fluid, have a unique effect on the system efficiency at part load, when compared to air. The water continues to circulate when the compressor is off, heating/cooling the zone beyond its set-point temperature limits. The thermal inertia of the secondary fluid can cause difficulty in maintaining zone set-point temperature; this would be further complicated by variable speed control. Riviere (2004) also concluded that an increase in the volume of water in the secondary circuit could reduce the efficiency of the heat pump by degrading the temperature stability. Karlsson and Fahlen (2007) optimised the pump flowrate for maximum system COP. The optimised pump flowrate depends on the circulation pumps, compressor and heat exchanger characteristics as well as the desired heat load to be delivered. An optimisation algorithm was used to adjust the pump flowrate depending on the conditions. It was concluded that power savings in the circulation pumps can only be realised if the decrease of compressor power is larger than the increase in power to the circulation pumps.

2.3. Temperature setback and bandwidth control

Temperature setback involves controlling the zone or supply water temperature depending on factors including the outside temperature, occupancy profile or tariff rates to maintain comfort and reducing energy usage. In a study by Albieri et al (2008) on/off compressor control for cooling was tested using one of three control parameters: building supply temperature, building return temperature and floating set-point of the supply temperature. Floating set-point control operates by increasing the supply temperature set-point for decreasing part load ratios and it was shown to give the highest COP when compared with the other two methods.

A number of studies have investigated scheduled set-point control using passive thermal energy storage. Using this control method, the thermal mass of a building can be charged during off peak times. For thermal storage control to be effective detailed knowledge of the heating system, energy storage potential of the structure and predicted weather conditions is needed. If this information is not known, scheduled set point control can lead to an increase in cost. In a study by Henze et al (2006), pre-cooling was initiated for off peak times. An optimisation algorithm utilising predicted data was used to select the pre-cooling times. This strategy was tested using simulation software and it was observed that although the total power usage increased the total energy cost decreased by 13%. The set-point temperature bandwidth was also increased during unoccupied times. In cooling applications, the cooler outside air at night results in an increase in COP, along with the reduced tariff rate, however the opposite would be true for pre-heating. The set-point can also be actively controlled depending on the current weather, occupancy and indoor temperature conditions. This form of control does not require predicted information.

Chen (2000) generated weather predictions from current and past weather data for an under-floor heating system. The set-point was optimised to reduce cost according to the utility rate. The indoor temperature bandwidth was also reduced during occupied times. Ma and Wang (2009), Braun (2007), Spindler and Norford (2008) and Zaheer-uddin and Zheng (1999) also noted positive results when using temperature set-back and thermal energy storage.

2.4. Heat pump simulation models

A number of studies concerned with heat pump control use validated simulation models of the heat pump system to accelerate testing of control strategies. These models consist of the heat pump, internal and external hydronic loop with components, ground and building models. However, the type and complexity of model used can vary substantially. Two broad categories of simulation models exist, empirical and analytical (Sreedharan, 2001).

Empirical models are data driven and typically include polynomial fit curves and in some cases artificial neural networks (ANN). They relate the inputs to the outputs of the system using equations not based on knowledge of the actual physical system. Their accuracy relies on the amount and scope of data supplied. Because of this they cannot be generated for a system that has not yet been installed and tested. Manufacturer's data and experimental results are used to create polynomial fit curves. Shao et al (2004) used performance fit curves to characterise the mass flowrate of refrigerant, capacity and power required for a variable speed compressor using manufacturer information. This was done for selected compressor frequencies and the performance at intermittent frequencies was interpolated. Similarly Karlsson and Fahlen (2003) and Zhou *et al* (2005) used polynomial curves to characterise the components of a heat pump system. The curve equations expressed the desired output in terms of measurable system variables such as the inlet/outlet temperatures of the heat pump and the mass flow-rate of primary or secondary fluids. A quasi-steady state analysis is usually used for these models. Heat pump and hydronic system models developed in studies including Cui et al, (2008) and Sakellari et al, (2006) were also linked to building modelling software. Outlet temperatures and flowrates were sent as inputs to the software and return water values were reported as input to the heat pump model.

In studies by Esen et al, (2007) and Esen and Inalli (2009) ANNs were used to characterise the performance of a heat pump. The inputs and outputs to an ANN model are similar to those used in polynomial fit curves but differ as the inputs/outputs are linked automatically by the program. The limitation with this type of modelling is that it has no knowledge of the system and requires large amounts of

data for accuracy. Inaccuracies may also be observed when testing conditions beyond the scope of the experimental data (Spindler and Norford 2008).

Analytical models are based on physical models that rely on established scientific equations (Spindler and Norford 2008). One benefit is that they can be used to guide design of a system that has not yet been installed, therefore changes to the system can be easily tested. These models may also need to be calibrated using physical data because the inefficiency of complex processes are not fully accounted for with the idealised equations. A variable speed compressor was modelled by Cuevas and Lebrun (2009) using equations derived from refrigerant flow characteristics within the compressor which also allowed for inverter evaluation. Other models, such as those developed by Ma and Wang (2009), Albieri et al (2008) and Yang and Pedersen (2007) use more fundamental equations based on thermodynamic principles to model the heat pump system components. Simulation software (which contains inbuilt equations) can also be used to aid with building, heat pump and ground modelling. Gamberi et al (2009) used Simulink simulation package to model a boiler based hydronic heating system for a typical building heating circuit.

3. METHODOLOGY

3.1. Description of the scope of a potential physical system

The heat pump mathematical model was conceptualised with the capability of capturing the behaviour of each component while avoiding unnecessary complexity. It was designed in a generalised form so that it could be easily adapted for different system characteristics. These characteristics could include changes in the heat-pump system and building circuits along with changing weather and ground conditions.

To provide for a generalised mathematical model and associated simulation code, the heat pump and hydronic system components were analysed and modelled individually. This was done to ease with integration of individual components for different heat pump systems. Specifically, potential changes associated with exchange of heat pump, circulation pumps, hydronic pipe work, secondary fluid tanks, bore holes and fan coils were all considered. A typical layout of a conceptual generalised heat pump system is shown in Figure 3.1

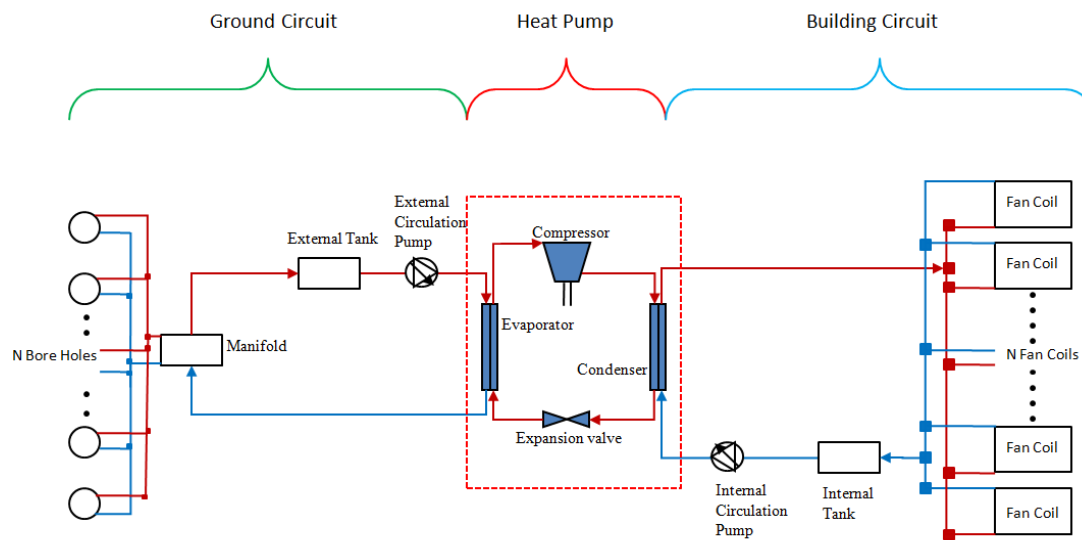


Figure 3.1 Generalised Heat Pump System

3.2. Performance characterisation of heat pump system

For the purposes of this research, it was decided to model the heat pump and hydronic system components by establishing performance maps using fitted correlations determined either from data obtained by experimental means or from manufacturer

performance specifications. The performance maps utilised in this work have some similarities to those constructed in studies by Esen *et al.*, (2007) and Gamberi *et al.*, (2009). Gamberi focussed on modelling a hydronic heating system, albeit in a boiler system, whereas Esen considered the application of neural networks, for a heat pump system. Performance correlations were utilised for each of the heat-pump, circulation pump and fan-coil models. Other circuit components such as the hydronic pipeline, tank and conditioned space were modelled using fundamental thermodynamic equations. Component models were created based on a sample system and applied to the simulation code for evaluation. The following sections describe the development of each component model in detail.

3.2.1. Heat pump model

The specification of the performance correlations of the heating and cooling capacity as well as compressor power consumption of a sample heat pump is explained in this section. This was achieved through the use of IMST-ART (Corberan *et al.*, 2002) and EXCEL software programs. By incorporating manufacturer's performance data and dimensional data for each heat pump component, an accurate model of the heat pump using the IMST-ART can be constructed. Heating and cooling mode performance correlations can be obtained using EXCEL polynomial curve fitting regression method. This was achieved by applying the curve fit application to a set of IMST-ART steady-state simulation result. The heat pump performance correlations take the form of multivariable functions and consist of the following four independent variables as follows:

- Volume flow-rate of water through the internal circuit (V_{CI})
- Volume flow-rate of water through the external circuit (V_{CE})
- Return water temperature from the fan coils (T_{RCI})
- Return water temperature from the ground loops (T_{RCE})

If written in equation form, these relations can be expressed generally as follows:

$$\dot{Q}_{\text{evaporator}} = f(V_{CI}, V_{CE}, T_{RCI}, T_{RCE}) \quad (1)$$

$$\dot{Q}_{\text{condenser}} = f(V_{CI}, V_{CE}, T_{RCI}, T_{RCE}) \quad (2)$$

$$\dot{P}_{\text{compressor}} = f(V_{CI}, V_{CE}, T_{RCI}, T_{RCE}) \quad (3)$$

Equations 4, 5 and 6 represent the correlations that were found to be most suitable for prediction of evaporator and condenser capacity compressor and the power consumption based on the four variables for cooling mode. An error minimisation approach was taken to formulate an equation that best describes the relationship between each variable and the performance characteristic of the heat pump component in question.

Cooling Mode Correlations

$$\dot{Q}_{\text{evaporator}} = A_0 + (A_1 * V_{\text{CE}}) + (A_2 * V_{\text{CE}}^2) + (B_1 * V_{\text{CI}}) + (B_2 * V_{\text{CI}}^2) + (C_1 * T_{\text{RCI}}) + (C_2 * T_{\text{RCI}}^2) + (D_1 * \frac{T_{\text{RCE}}}{T_{\text{RCI}}}) + (D_2 * V_{\text{CI}} * T_{\text{RCI}}) \quad (4)$$

$$\dot{Q}_{\text{condenser}} = A_0 + (A_1 * V_{\text{CE}}) + (A_2 * V_{\text{CE}}^2) + (B_1 * V_{\text{CI}}) + (B_2 * V_{\text{CI}}^2) + (C_1 * T_{\text{RCE}}) + (C_2 * T_{\text{RCE}}^2) + (D_1 * \frac{T_{\text{RCE}}}{T_{\text{RCI}}}) + (D_2 * V_{\text{CI}} * T_{\text{RCI}}) \quad (5)$$

$$\dot{P}_{\text{input}} = A_0 + (A_1 * V_{\text{CI}}) + (A_2 * V_{\text{CI}}^2) + (B_1 * V_{\text{CE}}) + (B_2 * V_{\text{CE}}^2) + (C_1 * T_{\text{RCI}}) + (C_2 * T_{\text{RCI}}^2) + (D_1 * T_{\text{RCE}}) + (D_2 * T_{\text{RCE}}^2) + (E_1 * T_{\text{RCI}} * V_{\text{CE}}) \quad (6)$$

where $A_0, A_1, A_2, B_1, B_2, C_1, C_2, D_1, D_2$ and E_1 are coefficients.

Using these equations and the IMST-ART simulation results, the coefficients of each equation can be determined. To assess whether the equations resulted in an accurate curve fit compared to the IMST ART data, a regression analysis was conducted. For each of the three correlations in cooling mode (Equations 4,5 and 6) it can be seen that the least accurate curve fit (power consumption) exhibits an error not greater than 0.6%, as shown in Figure 3.2. Figure 3.2 also shows the effect of varying the circulation pump speeds on the heat pump power consumption. Correlation curves for evaporator/condenser capacity and power consumption in heating mode can also be determined.

3.2.2. Circulation pumps

The circulation pumps control the flow of the secondary fluid through the internal and external circuits. The model allows for an inverter to be utilised with each circulation pump. Pump speeds for any range of frequencies are potentially possible, once pump and inverter performance curves are available. The mass flowrate of the secondary fluid is estimated as a function of pump speed, which is specific to each hydronic circuit. This correlation can be determined on the basis of experimental data collected for each site installation. To evaluate the performance of the inverter when used in conjunction with the circulation pumps, a correlation for inverter efficiency against pump

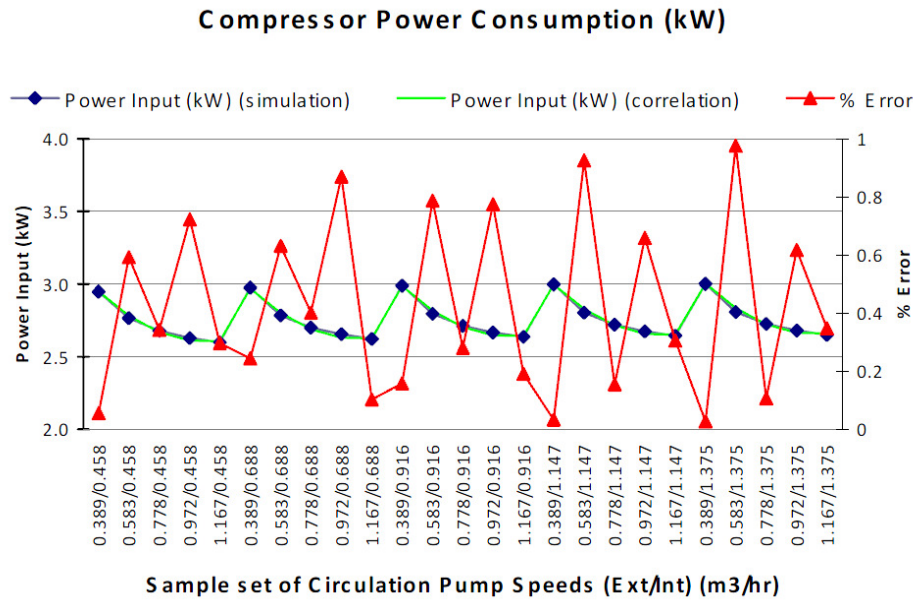


Figure 3.2 Comparison of compressor power consumption predictions (IMST-ART) and correlated data fit.

frequency is utilised as indicated by Equation 7. This correlation is determined by experimental testing of the inverter or from data from the manufacturer.

$$\text{Inverter efficiency} = [F_1(F_{REQ})^2 + F_2(F_{REQ}) + F_0] / 100 \tag{7}$$

The pump affinity laws are used to obtain the variation of pump head, pump capacity and electrical power consumption as a function of pump speed. For application of the affinity laws, data based on nominal pump speeds (50Hz) is deployed. A typical circulation pump performance correlation is shown in Figure 3.3

3.2.3. Fan coil

In the current version of the mathematical model, each fan coil is assumed to be identical. Correlations are determined that express the UA value of each fan coil as a function of air and water mass flowrates. The volumetric flowrate of air was estimated from manufacturer data sheets for each fan coil. The fans are assumed to operate continuously whereas the heat exchangers operate intermittently. An auxiliary variable controls a three-way valve which diverts the flow of water to and from the fan coil heat exchanger unit according to demand. Space temperature is controlled by

a thermostat located in the conditioned space and the bandwidth and set-point of the temperature can be modified according to requirements.

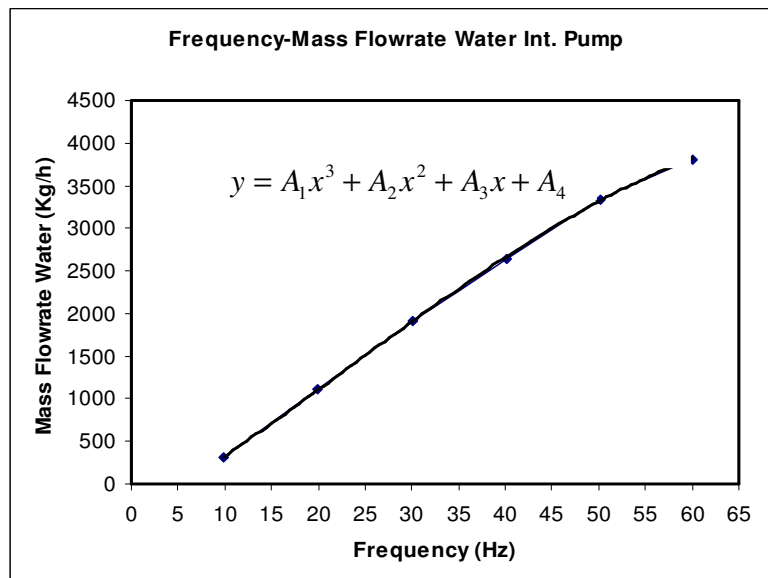


Figure 3.3 Circulation Pump Performance Correlation

In order to obtain the actual capacity of the fan coils for each operating condition, an experimental characterisation must be carried out to obtain the relationship between the fan coil UA value and water mass flowrate. Alternatively, this information may be available from the manufacturer. The fan coil UA value can be determined for each combination of water inlet temperature, water outlet temperature, ambient air temperature, air outlet temperature and air mass flowrate. A number of additional independent variables including the heat exchanger heat transfer and effectiveness are determined using the NTU approach. A typical fan performance relationship is given shown in Figure 3.4.

3.2.4. Hydronic pipe network

The internal hydronic circuit connects the heat pump refrigeration circuit with the building fan coil units. The network is modelled using the Lax-Wendroff model for 2D transport conduction using the Lax-Wendroff finite difference equation [Lax and Wendroff 1960]. The flow in the pipes is governed by the transport equation which can be written using the following partial differential equation:

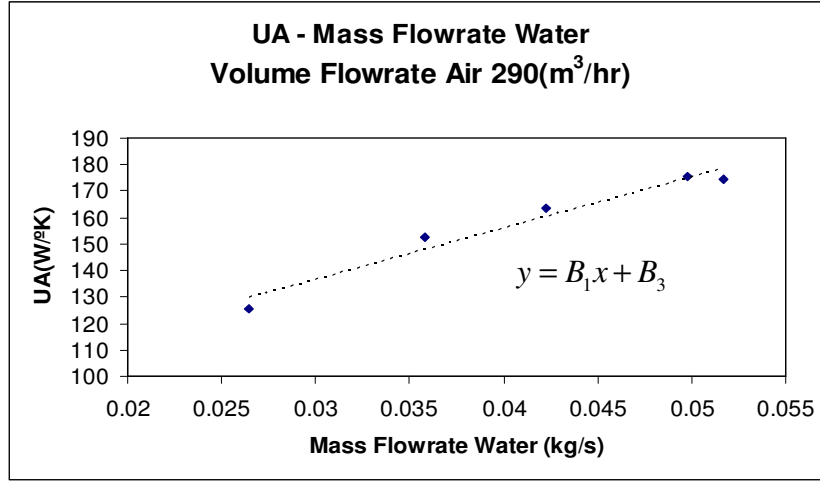


Figure 3.4 Fan Coil UA Correlation.

$$\frac{\partial T_{\text{water}}}{\partial t} = V_{\text{water}} \cdot \frac{\partial T_{\text{water}}}{\partial x} + \frac{P \cdot U}{\rho_{\text{water}} \cdot A \cdot C_{p\text{water}}} \cdot (T_{\text{water}} - T_{\infty}) \quad (8)$$

As the network is assumed to have negligible losses to the ambient, Equation 8 is simplified as follows:

$$\frac{\partial T_{\text{water}}}{\partial t} = V_{\text{water}} \cdot \frac{\partial T_{\text{water}}}{\partial x} \quad (9)$$

Equation 9 is a hyperbolic partial differential equation and it is solved using the Lax & Wendroff explicit discretisation approximation. This is governed by the Courant-Friedrichs-Lewy (CFL) condition, which is subject to the following constraint:

$$\Delta t \leq \frac{\Delta x}{v_{\text{water}}} \quad (10)$$

The CFL condition implies that for a given velocity of the water circulating in the pipes, the time step is controlled by the distance between the two consecutive nodes considered. The discretized version of Equation 9 can then be re-written as follows:

$$\frac{dT_{\text{water}}}{dt_i} = \frac{-v_{\text{water}}}{2 \cdot dx} \left[T_{\text{water}_{i+1}} - T_{\text{water}_{i-1}} - \left(\frac{T_{\text{water}_{i+1}} - 2 \cdot T_{\text{water}_i} + T_{\text{water}_{i-1}}}{dx} \right) \cdot v_{\text{water}} \cdot dt \right] \quad (11)$$

Solving gives an explicit solution for Equation 11 gives:

$$T_{\text{water}_i} = T_{\text{water}_{\text{initial},i}} + \int_0^{t,\text{final}} \left(\frac{dT_{\text{water}}}{dt_i} \right) dt \quad \text{for } i = 2 \text{ to } N-1 \quad (12)$$

3.2.5. Water storage tank

A mass balance is used to model the behaviour of the water in the tank. For modelling purposes, the storage tank is considered to be a single homogenous control volume with a single entry and a single exit, as given by Equation 13. Given that the tank is thermally insulated negligible heat losses are assumed, which allowed Equation 13 to be simplified to Equation 14

$$M_{\text{water}} \cdot C_{p\text{water}} \cdot \frac{dT_{\text{water}}}{dt} = \dot{m}_{\text{ICP}} \cdot C_{p\text{water}} \cdot (T_{\text{out,HP}} - T_{\text{water}}) + UA(T_{\text{water}} - T_{\infty}) \quad (13)$$

$$\frac{dT_{\text{water}}}{dt} = \frac{\dot{m}_{\text{ICP}} \cdot (T_{\text{out,HP}} - T_{\text{water}})}{M_{\text{water}}} \quad (14)$$

3.3. Building model characterisation

Each building space is modeled assuming a constant volume closed system as follows:

$$M_{\text{air}} c_{\text{pair}} \frac{dT_{\text{air}}}{dt} = \dot{Q}_{\text{FanCoil}} + \dot{Q}_{\text{load}} \quad (15)$$

where \dot{Q}_{FanCoil} is the heating/cooling capacity associated with the fan coil and is written as follows:

$$\dot{Q}_{\text{FanCoil}} = \dot{m}_{\text{air}} c_{\text{pair}} \epsilon_{\text{FC}} (T_{\text{air}} - T_{\text{in,water}}) \quad (16)$$

and \dot{Q}_{load} is the heating or cooling load associated with the space.

3.4. Ground model characterisation

The outdoor ground loop circuit consists of a circulation pump, an inverter, N ground loops and a small mixing tank. At this point there is no explicit code in the simulation for the outdoor ground loop circuit. The important variables from the outdoor ground loop circuit include the ground loop secondary fluid flowrate and the ground return temperature. Further work in Deliverable 4.2 will provide a more sophisticated model of the ground behaviour.

4 SIMULATION MODEL

This section describes the simulation model developed as part of GROUNDMED Deliverable 4.1. The overall model was developed using EES (Engineering Equation Solver) and is based on integration of the performance maps of each system component (heat pump, circulation pumps, fan coils) with the building hydronic circuit model and a building performance model.

4.1 System architecture

Figure 4.1 outlines the overall conceptual architecture of the simulation model. Performance maps are assumed to be available either by testing or from the manufacturer for the heat pump, the circulation pumps and the fans coils. Ground water return temperature is available from a separate analysis of the ground loop behaviour. Separate models of the hydraulic circuits, storage elements and building were developed to create a simulation framework for the system model.

4.2 Heat Pump model

The EES code developed for the heat pump was created using performance correlations that simulate performance in cooling or heating mode as described in Section 3. The evaporator and condenser capacity along with the compressor power consumption is capable of being predicted using the fitted correlations, subject to knowledge of building water return and ground water return temperatures and the building and ground mass flowrates. From this the secondary fluid temperatures exiting the heat pump for the internal and external circuits may be determined. For steady-state analysis, the results are directly calculated as the analysis is performed for a single time-step, whereas for quasi-steady state simulation, calculations are executed for each time-step based on a user-set amount of timesteps. Tables 4.1, 4.2 and 4.3 contain the code for the simulation of the heat pump in cooling and heating mode.

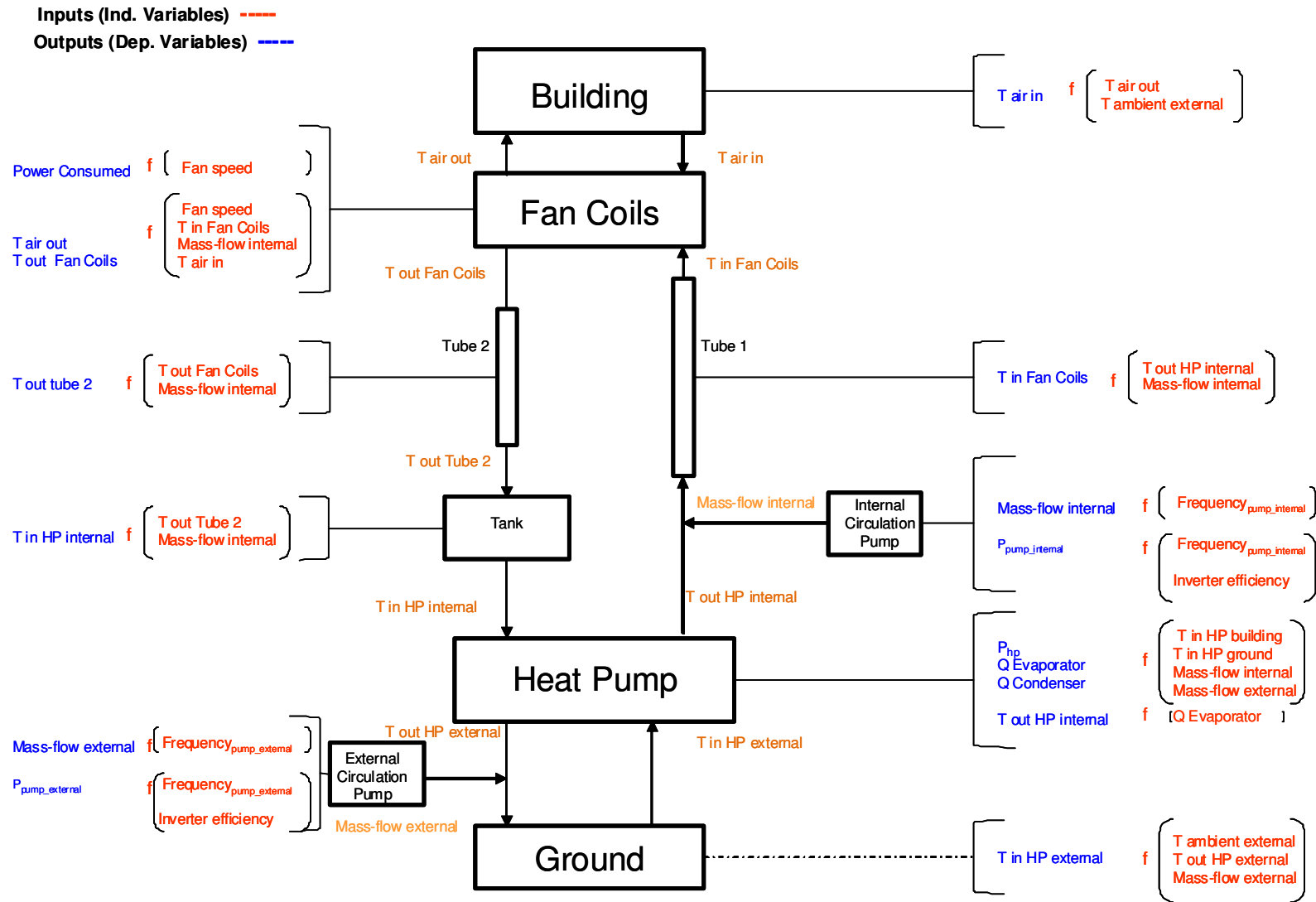


Figure 4.1 Conceptual Model Architecture

In Tables 4.1 and 4.2, it can be observed that the P_{input} terms are multiplied by the auxiliary variable 'Aux_HP' which is used in the quasi steady-state simulation. The on-off operation of the heat pump is governed by this variable and is controlled by a set-point temperature (T_{ret_HP}) and an associated upper/lower bandwidth temperature (Lines 9 and 10 in Table 4.3). The set-point temperature is measured on the internal circuit at the heat pump return. In cooling mode, if the secondary fluid temperature drops below the lower limit of the control temperature, ($T_{ret_HP_off}$), the auxiliary variable will be assigned a value of zero and the heat pump switches off on this condition. When the secondary fluid temperature exceeds the upper limit of the control temperature, ($T_{ret_HP_on}$), the auxiliary variable will be assigned a value of one and the heat pump will operate. The opposite applies to the operation of the heat pump in heating mode.

The energy imparted to or taken from the water passing through the heat exchanger is given by Equation 17. It calculates the change in temperature of the secondary fluid for one time-step. To identify the water temperature exiting the heat pump for each time-step, Equation 17 is integrated over time from t_0 to $t_{selected}$ and the result is added to the entering water temperature.

$$dT_{out,HP} = [(m_{ICP} * C_{p,water} * (T_{RCI} - T_{out,HP}) - Q_{HP}) / (M_{water} * C_{p,water})] \quad (17)$$

Heat Pump Model in Cooling Mode	Line
$Q_{HP} = Q_{evaporator}$	1
$P_{cons_HP} = P_{input} * Aux_HP$	2
$dT_{out_HP}/dt = (\text{Equation 11})$	3
$T_{out_HP} = T_{out_HP_initial} + \text{integral}(dT_{out_HP}/dt, t, 0, t_{final}, dt)$	4

Table 4.1 EES code for heat pump in cooling mode

Heat Pump Model in Heating Mode	Line
$Q_{HP} = Q_{condenser}$	5
$P_{cons_HP} = P_{input} * Aux_HP$	6
$dT_{out_HP}/dt = (\text{Equation 11})$	7
$T_{out_HP} = T_{out_HP_initial} + \text{integral}(dT_{out_HP}/dt, t, 0, t_{final}, dt)$	8

Table 4.2 EES code for heat pump in heating mode

Table 4.3 comprises of the properties of the working fluid (water) in the internal secondary circuit. It also contains the defined operating bandwidth of the secondary fluid temperature. The code from Tables 4.1 to 4.3 is used as a framework to develop a model of the building integrated ground source heat pump system.

Heat Pump Boundary Conditions and Water Properties	Line
$T_{ret_HP_on}=T_{ret_HP}+1.5$	9
$T_{ret_HP_off}=T_{ret_HP}-1.5$	10
$Rho_water_HP=999 [Kg/m^3]$	11
$Cp_water_HP=4.19 [KJ/Kg.K]$	12
$M_water_HP=V_water_HP*rho_water_HP$	13
$T_{ret}=T_{tank}$	14
$dT_{ret}/dt=dT_{tank}/dt$	15

Table 4.3 Heat pump boundary conditions and water properties

4.3 Circulation pumps

Tables 4.4 and 4.5 display the model code used to calculate mass flowrate and power consumption of the internal and external circulation pumps. The term ‘alpha’ is defined as the ratio of actual operating frequency to the nominal operating frequency (50Hz). The terms ‘mICP’ and ‘mECP’ represent the mass flowrate of water through the pumps. The equation for the power consumption of each pump was calculated using correlations from the pump manufacturer and is represented by the term ‘Pcons’ in the EES code. The inverter efficiency equation (line 21) is set for each circulation pump. The total power consumption of the unit can be calculated on the basis of the inverter efficiency and pump power consumption.

Internal Circulation Pump Model	Line
FUNCTION CalculatePowICP(Freq)	16
$alpha=Freq/50$	17
$mICP=(-0.0094*Freq^3+0.6414*Freq^3+65.323*Freq-380.86)/1000$	18
$mP=mICP/alpha$	19
$Pcons=(-11.447*mP^2+140.51*mP+338.72)*alpha^3$	20
$InverterEFF=(-0.0261*Freq^2+2.3335*Freq+43.765)/100$	21
$CalculatePowICP=Pcons/InverterEFF$	22
END	23

Table 4.4 Model of indoor hydronic circuit circulation pump in EES

External Circulation Pump Model	Line
FUNCTION CalculatePowECP(Freq)	24
alpha=Freq/50	25
mECP=(-0.0023*Freq^3+0.1279*Freq^2 +52.71*Freq-54.067)/1000	26
mP=mECP/alpha	27
Pcons=(-8.7555*mP^2+88.958*mP+261.73)*alpha ³	28
InverterEFF=(-0.0261*Freq^2+2.3335*Freq+43.765)/100	29
CalculatePowECP=Pcons/InverterEFF	30
END	31

Table 4.5 Model of outdoor ground loop circulation pump in EES

4.4 Fan coil

The fan coils are modelled using correlations constructed from experimental or manufacturer's data. The associated EES code is illustrated in Table 4.6. The units are assumed to be connected in parallel. This results in the water supply to the fan coils being split equally into parallel flow-paths (Line 32 in Table 4.6). The water temperature entering the fan coils is assigned the same value as that exiting the pipe connecting the heat pump and coils. The maximum and minimum capacities of each media (air and water) involved in heat transfer across the fan coil are calculated. Line 34 applies the approach to each fan coil unit. In this case, the fan coil units have three separate ventilation speeds. These speeds are defined in EES as a 'Procedure'. This procedure is called forward (Line 47) to define the UA-value of the heat transfer process associated with each fan coil for each set fan speed. The operation of the fan coil unit is based on a set-point temperature and bandwidth control using a thermostat in the conditioned space. In cooling mode, when the lower limit temperature is attained, the water in the circuit is re-routed for that fan coil directly back to the heat pump. The conditioned space begins to heat until the corresponding upper limit temperature has been exceeded. The water will be directed back through the fan coil when the room temperature rises above the upper bandwidth to resume cooling. A similar procedure is performed in heating mode. The NTU of the fan coils and their effectiveness are calculated in Lines 48 and 49 in Table 4.7. The heat transfer from the water in the coil to the air in cross-flow is also calculated. This enables EES to calculate the temperature of the air exiting the ventilation system in addition to the temperature of the water exiting the fan coil for any time-step (Lines 50 & 51 in Table 4.8). The capacity of each fan coil unit based on the properties of the air and water

passing through the units and is also calculated using equations shown in Table 4.8. Table 4.9 shows how the total capacity of the fans and the total power consumed by each fan coil units is calculated. After passing through the fan coils, the return water from the fan coils mixes before it enters the water storage tank. Line 4.59 calculates the final temperature of the return water from the fan coils as it enters the tank.

Air and Water Properties for Fan Coil model	Line
$m_dot_water_fan = m_dot_ICP / N_{coils}$	32
$T_in_water_fan = T_1[N_1]$	33
Duplicate $i=1, N_fans$	34
$T_in_air_fan[i] = T_air_room[i]$	35
$Cp_air_fan[i] = 1.005 [KJ/Kg.K]$	36
$Cp_water_fan[i] = 4.19 [KJ/Kg.K]$	37
$C_air_fan[i] = m_dot_air_fan[i] * Cp_air_fan[i]$	38
$C_water_fan[i] = m_dot_water_fan * Cp_water_fan[i]$	39
$C_max_fan[i] = MAX(C_air_fan[i], C_water_fan[i])$	40
$C_min_fan[i] = MIN(C_air_fan[i], C_water_fan[i])$	41
$Rc_fan[i] = C_min_fan[i] / C_max_fan[i]$	42
$\rho_air_fan[i] = 1.166 [Kg/m^3]$	43
$\rho_water_fan[i] = 999 [Kg/m^3]$	44
$M_water_fan[i] = V_water_fan * \rho_water_fan[i]$	45
$M_air_fan[i] = V_air_fan * \rho_air_fan[i]$	46
call Fan_coils(Fan_Speed[i], m_dot_water_fan: V_air_fan[i], UA_fan[i])	47

Table 4.6 Water and Air heat transfer properties

NTU and Effectiveness Equations for Fan Coils	Line
$NTU_fan[i] = UA_fan[i] / C_min_fan[i]$	48
$Epsilon_fan[i] = (1 - EXP((NTU_fan[i]^0.22 * (EXP(Rc_fan[i]) * NTU_fan[i]^0.78) - 1)) / Rc_fan[i])) * Aux_fans[i]$	49

Table 4.7 Calculation of NTU and effectiveness of fan coil units

4.5 Water storage tank

The EES code used to model the water tank is summarised in Table 4.10. The rate of change of temperature in the tank is dictated by the amount of energy contained in the water entering and leaving the tank (Lines 63 and 64 in Table 4.10). The cooling/heating demands of the heat transfer process on the water as it passes through the fan coils, together with the water flowrates, control the amount of energy contained in the tank.

Exit Temperature/Energy of Water and Air from Fan Coils	Line
$dT_{out_water_fan}/dt[i]=(Q_{water_fan}[i]-Q_{fan}[i]) / (M_{water_fan}[i]*Cp_{water_fan}[i])$	50
$dT_{out_air_fan}/dt[i]=(Q_{fan}[i]+Q_{air_fan}[i]) / (M_{air_fan}[i]*Cp_{air_fan}[i])$	51
$Q_{fan}[i]= Epsilon_{fan}[i]*C_{min_fan}[i]*(T_{in_water_fan}-T_{in_air_fan}[i])$	52
$Q_{air_fan}[i]=m_{dot_air_fan}[i]*Cp_{air_fan}[i]* (T_{in_air_fan}[i]-T_{out_air_fan}[i])$	53
$Q_{water_fan}[i]=m_{dot_water_fan}*Cp_{water_fan}[i]* (T_{in_water_fan}-T_{out_water_fan}[i])$	54
$T_{out_water_fan}[i]=T_{out_water_fan_initial}+ integral(dT_{out_water_fan}/dt[i], t, 0, t_{final}, dt)$	55
$T_{out_air_fan}[i]=T_{out_air_fan_initial}+ integral(dT_{out_air_fan}/dt[i], t, 0, t_{final}, dt)$	56

Table 4.8 Calculation of water/air temperature and energies across fan coil units

Total Power Consumption and Capacity of Fan Coils	Line
$Q_{fans}=ABS(SUM(Q_{fan}[i], i=1, N_{fans}))$	57
$P_{cons_fans}=ABS(SUM(P_{cons_fan}[i], i=1, N_{fans}))$	58
$T_{out_water_bat}=(1-N_{fans}/12)*T_{in_water_fan} + SUM(T_{out_water_fan}[i]/12, i=1, N_{fans})$	59

Table 4.9 Calculation of total capacity/ total power consumption of fans

Calculation of Water Temperature Evolution in Tank	Line
$\rho_{water_tank}=999 [Kg/m^3]$	60
$Cp_{water_tank}=4.19 [KJ/Kg.K]$	61
$M_{tank}= V_{tank}*\rho_{water_tank}$	62
$dT_{tank}/dt = (m_{dot_ICP}*Cp_{water_tank}*(T_{2[N_2]}-T_{tank})) / (M_{tank}*Cp_{water_tank})$	63
$T_{tank}=T_{tank_initial}+integral(dT_{tank}/dt, t, 0, t_{final}, dt)$	64

Table 4.10 Calculation of water temperature evolution in the water storage tank

4.6 Hydronic Pipe Network

The energy transported through the hydronic network by the circulated water is simulated using two-dimensional conduction finite difference method equations. The pipes are defined in terms of radii, cross-sectional area and length. The velocity of the water passing through them is then calculated by employing Lines 68 and 78 in Tables 11 and 12. There are two lengths of pipes in the water circuit, ‘PIPE 1’ and ‘PIPE 2’. Each tube is divided into N discrete sections or nodes. ‘PIPE 1’ connects the heat pump to the fan coils. The link from the heat pump to ‘PIPE 1’ is shown in Line 4.69. Lines 70 to 74 determine the temperature change in each node for a given timestep and add the value to the previous temperature.

Model of Water Temperature Evolution in Tube 1	Line
$\rho_{\text{water_pipe_1}}=999 \text{ [Kg/m}^3\text{]}$	65
$A_{\text{pipe_1}}=(\pi*D_{\text{Pipe_1}}^2)/4$	66
$dx_1= L_{\text{Pipe_1}}/N_1$	67
$vel_1=m_{\text{dot_ICP}}/(\rho_{\text{water_pipe_1}}*A_{\text{pipe_1}})$	68
$T_1[1]=T_{\text{out_HP}}$	69
Duplicate $i=2, N_1-1$	70
$dT_1/dt[i] \quad dT_1/dt[i]=(-vel_1/(2*dx_1))*(T_1[i+1]-T_1[i-1]-((T_1[i+1]-2*T_1[i]+T_1[i-1])/dx_1)*vel_1*dt)$	71
$T_1[i]=T_1_{\text{initial}}[i] + \text{integral}(dT_1/dt[i], t, 0, t_{\text{final}}, dt)$	72
$dT_1/dt[N_1]=(-vel_1/dx_1)*(T_1[N_1]-T_1[N_1-1])$	73
$T_1[N_1]=T_1_{\text{initial}}[N_1] + \text{integral}(dT_1/dt[N_1], t, 0, t_{\text{final}}, dt)$	74

Table 4.11 Mathematical description of temperature evolution of water travelling through Pipe_1

This method is also used to describe the transport of water through ‘PIPE 2’. ‘PIPE 2’ connects the fan coils to the water storage tank on the return path to the heat pump. Node 1 of ‘PIPE 2’ is located at the exit from the fan coils and node N is located at the entrance to the water storage tank.

Model of Water Temperature Evolution in Tube 2	Line
$\rho_{\text{water_tube_2}}=999 \text{ [Kg/m}^3\text{]}$	75
$A_{\text{tube_2}}=(\pi*D_{\text{tube_2}}^2)/4$	76
$dx_2= L_{\text{Tube_2}}/N_2$	77
$vel_2=m_{\text{dot_ICP}}/(\rho_{\text{water_tube_2}}*A_{\text{tube_2}})$	78
$T_2[1]=T_{\text{out_water_bat}}$	79
Duplicate $i=2, N_2-1$	80
$dT_2/dt[i] \quad dT_2/dt[i]=(-vel_2/(2*dx_2))*(T_2[i+1]-T_2[i-1]-((T_2[i+1]-2*T_2[i]+T_2[i-1])/dx_2)*vel_2*dt)$	81
$T_2[i]=T_2_{\text{initial}}[i] + \text{integral}(dT_2/dt[i], t, 0, t_{\text{final}}, dt)$	82
$dT_2/dt[N_2]=(-vel_2/dx_2)*(T_2[N_2]-T_2[N_2-1])$	83
$T_2[N_2]=T_2_{\text{initial}}[N_2] + \text{integral}(dT_2/dt[N_2], t, 0, t_{\text{final}}, dt)$	84

Table 4.12 Mathematical description of temperature evolution of water travelling through PIPE 2

The tank is located at the entrance to the indoor hydronic circuit heat exchanger. Therefore the properties of the water at the exit from the storage tank are assumed to be equal to those of the water at the entrance to the heat exchanger.

4.7 Building model

A simple control volume approach has been taken to describe the sensible heat gains in the building. As can be seen from Table 4.13, Line 86 describes the sensible heat loss from (or gain to) the space. Lines 91 and 92 describe the temperature evolution in each space according to the interaction of the fan-coil units with the air in the rooms. By integrating Line 91 at any instant during the simulation from time $t=0$ until $t=final$ and integrating with respect to the initial room temperature, the current room condition can be calculated (Line 92).

Model of Energy Balance in Conditioned Space	Line
Duplicate $i=1, N_fans$	85
$Q_room[i]=UA*(T_amb_ext - T_air_room[i])+0.2$	86
$Q_total_building=ABS(SUM(Q_room[k], k=1, N_fans))$	87
$\rho_air_room[i]=1.166 [Kg/m^3]$	88
$Cp_air_room[i]=CAPITANCE_FACTOR*1.005 [KJ/Kg.K]$	89
$M_air_room[i]=V_room*\rho_air_room[i]$	90
$dT_air_room\ dt[i]=(Q_room[i]-Q_air_fan[i])/$ $(M_air_room[i]*Cp_air_room[i])$	91
$T_air_room[i]=T_air_room_initial+ \text{integral}(dT_air_room\ dt[i], t, 0, t_final,$ $dt)$	92

Table 4.13 Model of energy balance in the conditioned space

4.8 Initialising System Variables

Table 4.14 displays the initial values of the variables of the system and how they are connected. The variable 'T_initial' (Line 114) is assigned a value by the user. By inspecting Table 4.14 one can follow how the initial temperature of the water and air throughout the model is assigned using the original 'T_initial' value.

4.9 Execution of EES simulation

EES operates on an integration basis over a user set period of time. The checkstop function in Table 4.15 enables the user to set the required duration of the simulation (Line 4.127). When the simulation exceeds the set time limit, a value of 1 is assigned to the checkstop function and the simulation terminates.

Variable	Description	Line
T_air_room_initial=308 [K]	Initial room temperature	113
T_initial=308 [K]	Initial temperature of the water in the circuit pipes and fan coils	114
T_out_water_fan_initial=T_initial	Initial temperature of the water exiting the fan coils	115
T_out_air_fan_initial=T_air_room_initial	Initial temperature of the air exiting the fan coils	116
T_out_HP_initial=T_initial	Initial temperature of the water exiting the HP	117
T_tank_initial=T_initial	Initial temperature of the tank Initial temperature of the tank	118
T_1_initial[1]=T_out_HP_initial	Initial temperature of the first node in tube 1	119
Duplicate i=2, N_1	Duplicate conditions from node 1-12	120
T_1_initial[i]=T_initial	Initial temperature of the nodes in tube 1	121
T_2_initial[1]=T_out_water_fan_initial	Initial temperature of the first node in tube 2	122
Duplicate i=2, N_2	Duplicate node 1-12 conditions from	123
T_2_initial[i]=T_initial	Initial temperature of the nodes in tube 2	124

Table 4.14 Initial variable values for EES model

Checkstop Funtion (control of simulation duration)	Line
FUNCTION checkstop (t_min)	125
checkstop=1	126
IF (t_min>1440) THEN Call Error ('Simualtion has finished (Time of operation = 24 hours)')	127
END	128

Table 4.15 Checkstop function governing simulation duration

EES is an integration based program. In order to ensure convergence, it is necessary to set a suitable timestep for the integration process. The timestep criteria for the simulation are based on a function of the velocity of the water travelling through Tube 1 or 2 and the node length of each tube (Line 129 in Table 4.16).

Timestep and convergence criteria	Line
Dt=MIN(0.99*(dx_1/vel_1), 0.99*(dx_2/vel_2))	129
t_final=100000	130
t_min=t/60	131
Stop= integral(checkstop(t_min), t, 0, t_final, dt)	132

Table 4.16 Definition of the simulation time-step and convergence criteria in EES

5 SIMULATION MODEL CAPABILITIES AND RESULTS

The EES simulation model is capable of generating results as follows:

- Steady state performance: the heating/cooling capacity, compressor power consumption, system power consumption, COP_{hp} and COP_{sys} can be simulated.
- Transient time simulation data: the effect of varying the set-point and bandwidth values of the internal circuit water and room air temperature on the transient performance can be generated.
- Sensitivity analysis: the role of various independent control parameters on system dependent variables can be systematically examined by means of sensitivity studies.
- Time Integrated Analysis: the total energy consumption and heating/cooling capacity over a period of time, ranging from hours to months, can be compiled for comparison of different control strategies.

5.1 Steady state performance

Simulations were carried out to test the performance of the system model under steady state and quasi-steady conditions. The steady state performance was tested using the heat pump and circulation pumps only. A sample of the results for the analysis is shown. In order to examine the steady state performance of the heat pump system, certain assumptions were applied. This allowed heat pump performance maps to be determined as a function of hydronic circuit independent variables (i.e., water return temperatures and water fluid circulation rates).

Boundary conditions in heating mode:

- Internal circuit inlet water return temperature to condenser = 40°C
- External circuit inlet water return temperature to evaporator = 12°C
- Internal and external circulation pump frequencies = 10 to 70Hz

Boundary conditions in cooling model:

- Internal circuit inlet water return temperature to evaporator = 12°C
- External circuit inlet water return temperature to condenser = 23°C
- Internal and external circulation pump frequencies = 10 to 70Hz

Figure 5.1 shows how the heating and cooling capacity of the heat pump varies with changes in the internal and external pump frequencies. With respects to the heating capacity, when the flow-rate of water is increased through the condenser (internal pump), it results in an increased heat transfer co-efficient on the water side, resulting in an increase in the condenser U value. This leads to a decrease in the mean temperature difference across the condenser and a reduction in condenser saturation temperature. This results in a lowered condenser saturation pressure, which in turn leads to an increased condensing effect and associated heating capacity. The refrigerant mass flow-rate through the condenser is not significantly affected by the lowered condenser saturation pressure. Therefore, there is little effect on the heating capacity of the system with increasing secondary fluid flow-rates through the condenser. An increase in mass flow-rate of water through the evaporator (external pump) causes an increase in the value of the heat transfer co-efficient on the water side. This results in an increased mass flow-rate of refrigerant which lends to increased heating capacity of the heat pump. With increased mass flow-rate on the secondary side of the evaporator and an increases mass flow-rate of refrigerant through the compressor. This results in an increased heating capacity when compared to varying the internal pump frequency. The effect of varying the pump frequencies on the COP of the system (in heating mode) is shown in Figure 5.2. It can be seen that the maximum COP_{sys} exists at a combination of intermediate frequencies on the internal and external pumps. This is caused by a trade-off between an increase in the heating capacity and power consumption with increased pump frequency.

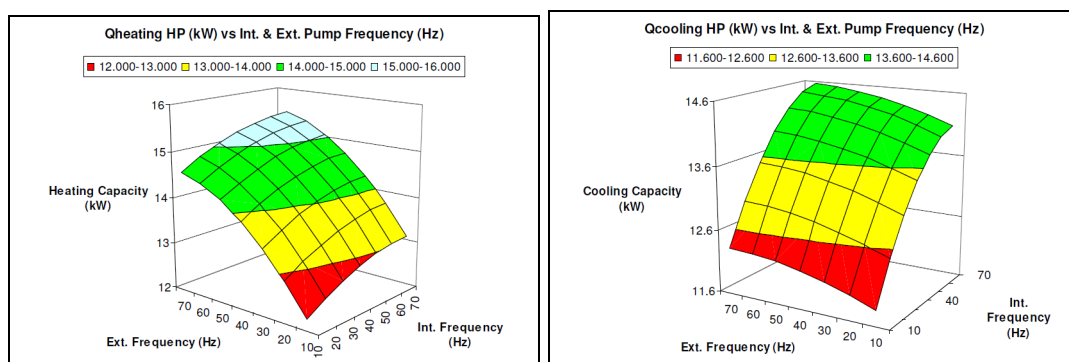


Figure 5.1 Heating capacity (left) and cooling capacity (right) vs. circulation pump frequencies.

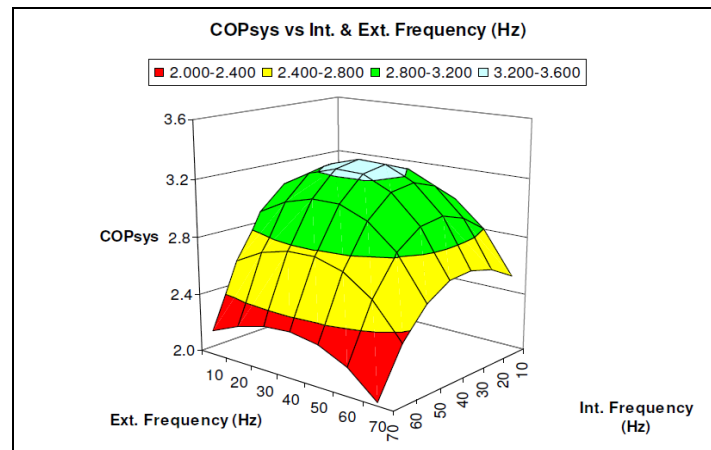


Figure 5.2 System COP vs circulation pump frequencies (heating mode).

5.2 Quasi-steady state performance

The heat pump is used to condition the building spaces and the spaces are subjected to internal and transmission load as a function of external ambient temperatures. A quasi-steady state simulation is illustrated in Figure 5.3 for cooling mode conditions.

The boundary conditions used in the simulation model were as follows:

- Space set-point temperature 23.5C
- Space temperature bandwidth ± 0.5 C
- Building return water set-point temperature 10.4C
- Building return water bandwidth ± 1.6 C
- Internal circulation pump frequency 60 Hz
- External circulation pump frequency 50 Hz

The simulation was run for a period of 24hrs and results are shown in Figure 5.3 from 0600 hrs to 2300 hrs. The building space temperature and the fan coil response are controlled by a room thermostat, where room load is governed by random occupancy patterns. Heat pump on-off control is based on a water return set-point temperature of 10.4C with a ± 1.6 C bandwidth.

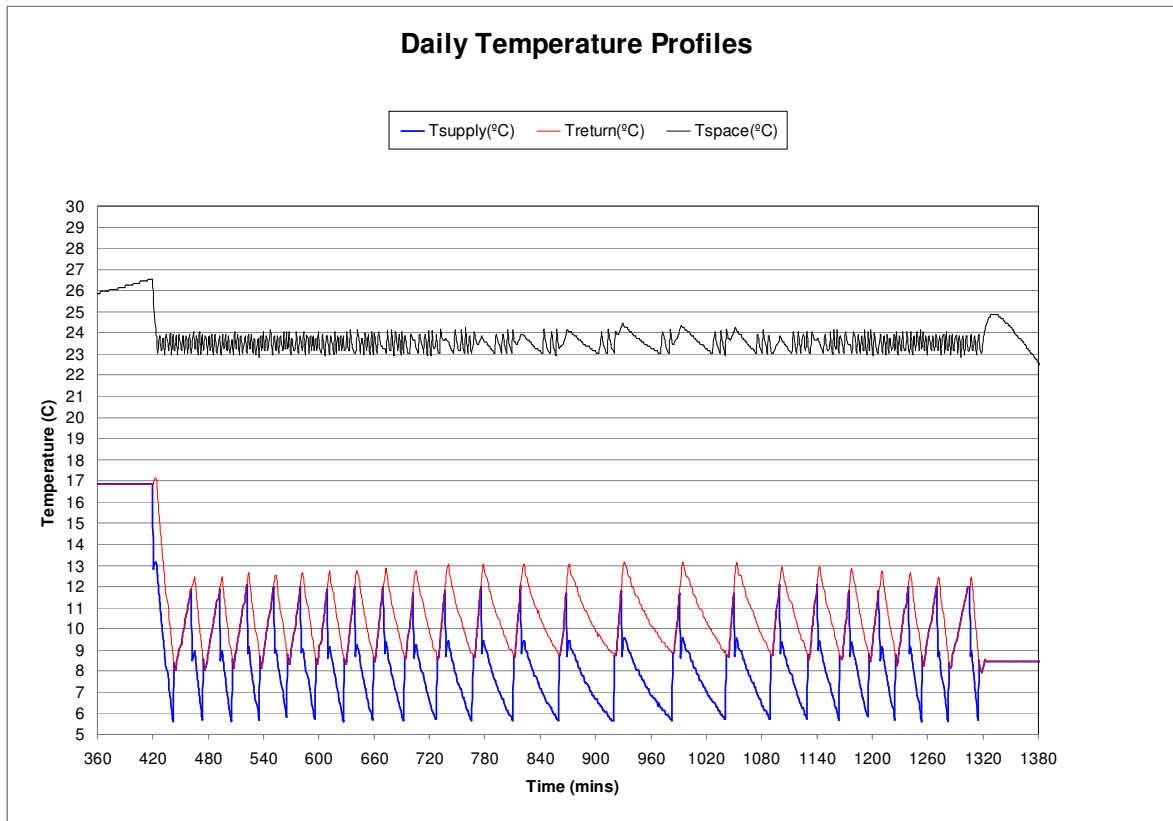


Figure 5.3 Daily profile of supply, return and space temperature (cooling mode).

5.3 Sensitivity Analysis

The model capabilities for sensitivity analysis of GSHP performance, subject to control of set-point temperature of the fan coil water return temperature and the space air temperature is demonstrated in this section. In addition, the role of bandwidth settings for the fan coil water return temperature and space air temperature are also considered. The sensitivity studies presented here are shown for cooling mode, the model is also capable of heating mode analysis, but for purposes of conciseness are not detailed in this report.

5.3.1 Sensitivity Study Boundary Conditions

For cooling mode analysis, the following reference boundary conditions were utilised:

- Space set-point temperature 23C
- Space temperature bandwidth ± 1 C
- Fan coil water return temperature 12C
- Fan coil water return temperature bandwidth ± 1 C

- Internal circulation pump frequency 60 Hz
- External circulation pump frequency 50 Hz

5.3.2 Set-point Control of Water Return Temperature

The effect of set-point control of building water return temperature are presented based on simulation analysis over a representative 24 hour period. Three water return temperatures, 10C, 12C and 14C were considered. All other system variables were constrained at the boundary conditions described in Section 5.3.1. Figure 5.4 illustrates the effect of different water return set-point temperatures on return temperature evolution for a typical 200 minute operational period of the system. It can be observed that, as the building water return set point temperature is increased from 10C to 14C, the heat pump compressor on-time decreases due to the increased cooling capacity associated with the underlying refrigeration cycle. Analysis shows that capacity increases by approximately 3.6% per degree increase of the building return water temperature.

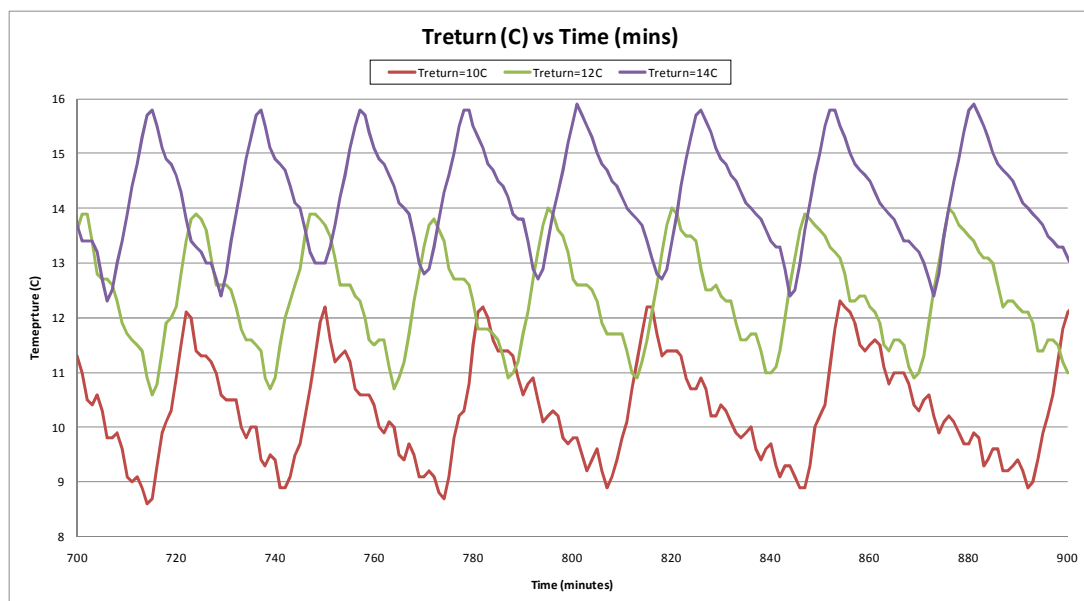


Figure 5.4 Building water return temperature evolution

5.3.3 Set-point Control of Space Temperature

Space temperature is controlled by an individual thermostat located in each space of the building. Three separate space set-point temperatures (21C, 23C and 25C) were analysed and the simulation predictions are shown in Figure 5.5. All other boundary conditions were maintained as outlined in Section 5.3.1. Space temperature set-point

is seen to have a significant influence on heat pump cyclic behaviour. An increase in space set-point temperature results in a decrease in the building heat gains. At higher space temperatures, due to the higher mean temperature difference between the space and the coil mean water temperature, a larger space to fan coil heat transfer load arises, and thus the water return temperature is observed to decrease faster during the heat pump on periods, given that the heat pump capacity remains constrained and is therefore unchanged. Thus for higher space set-point temperatures, the building water return temperature reaches the lower set-point temperature more quickly, resulting in a more frequent heat pump cycling associated with higher space temperature set-points.

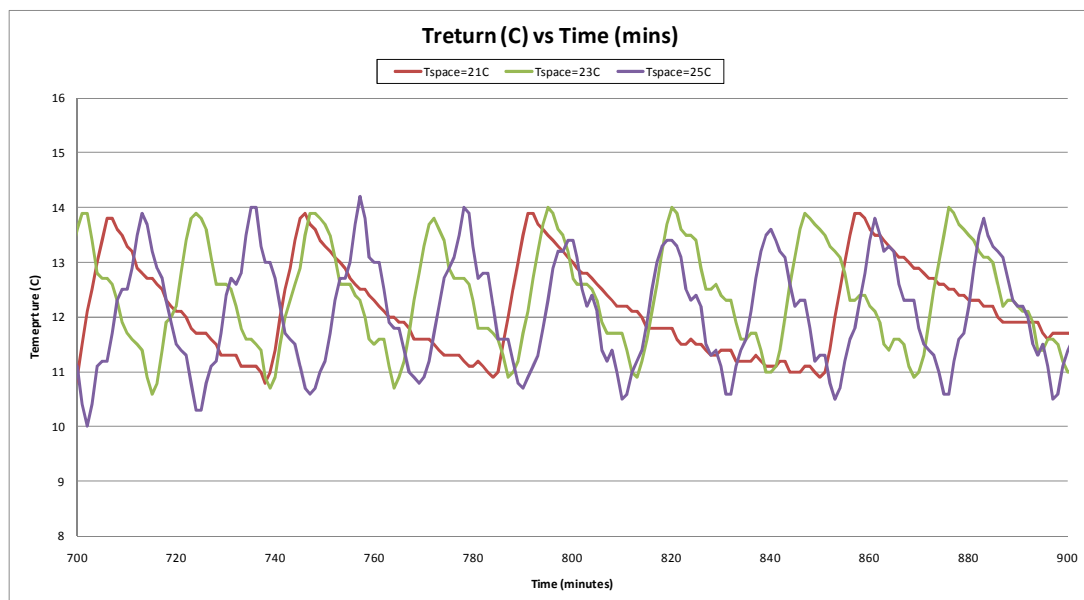


Figure 5.5 Set-point control of space temperature

5.3.4 Building Water Return Bandwidth

Bandwidth control for building water return temperature can be examined for different bandwidths, in this case bandwidths of $\pm 0.5\text{C}$, $\pm 1\text{C}$, $\pm 1.5\text{C}$, $\pm 2\text{C}$ are demonstrated. All other variables were maintained at the reference boundary conditions as outlined in Section 5.3.1. Reference to Figure 5.6 and Table 5.1 shows that changes in return water temperature appears to have a negligible effect on system performance characteristics. The ON time operation of the heat pump is not significantly affected by the return temperature bandwidth, so the heat pump energy consumption remains practically the same. In this case, total consumption would only be affected by the fan coils, but it also appears to be not significantly influenced by

changes in water return temperature bandwidth. Finally, examining Table 5.1, values for the SPF of the system and the heat pump are affected by less than 0.5% by return water temperature bandwidth.

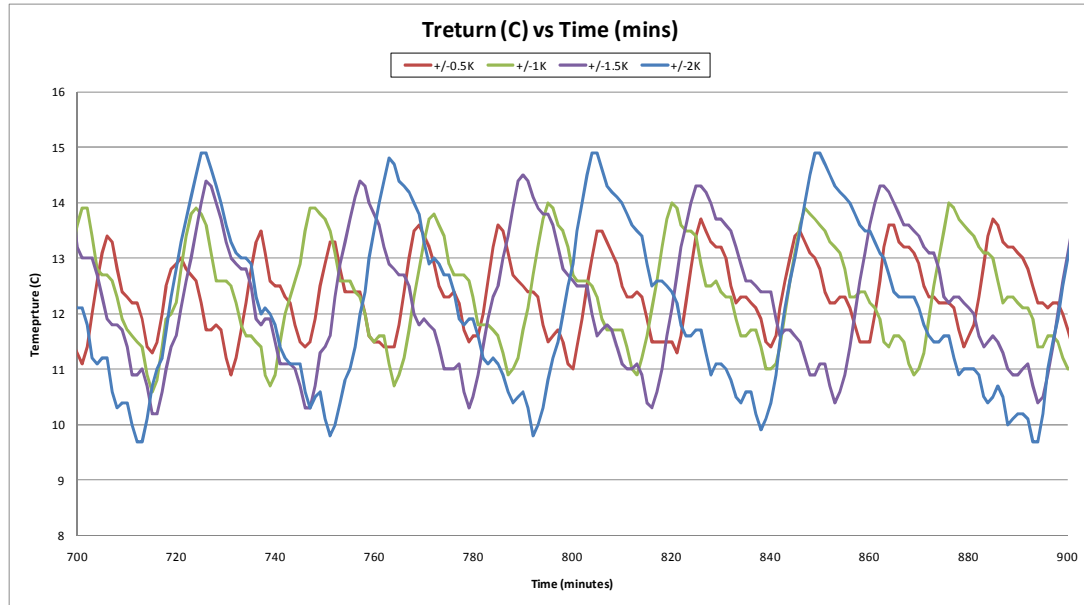


Figure 5.6 Building return temperature as a function of return water bandwidth

Building Water Return Bandwidth	±0.5C	±1C	±1.5C	±2C
HP ON (%)	40.04	39.97	39.90	40.39
HP OFF (%)	59.96	60.03	60.10	59.61
Energy Consumption - HP (kWh)	28.68	28.72	28.65	28.65
Energy Consumption - System (kWh)	58.35	58.40	58.32	58.32
Daily SPF of the HP	4.99	4.99	5.01	4.95
Daily SPF of the system	2.45	2.45	2.46	2.44

Table 5.1 System performance parameters as a function of return water bandwidth

5.3.5 Building Space Temperature Bandwidth

The role of space temperature bandwidth control can be considered and bandwidths of ±0.5C, ±1C and ±1.5C are evaluated in this report. Simulation results are given in Figure 5.5 and system performance is summarised in Table 5.2. For these results, a building space set-point temperature of 23C was used, along with the other boundary conditions given in Section 5.3.1 Examining Figure 5.5, it can be observed that

adjusting of the space temperature bandwidth has a modest effect on heat pump cyclic performance, as well as overall system performance. The ON time operation of the heat pump stays practically the same, which is why heat pump energy consumption remains constant. In this case, as total consumption is only be affected by the fan coils, it also appears to be insignificantly affected by changes in space bandwidth temperature as total consumption is practically constant. Finally, values for the SPF of the system and the heat pump are slightly affected less than 1% by space temperature bandwidth.

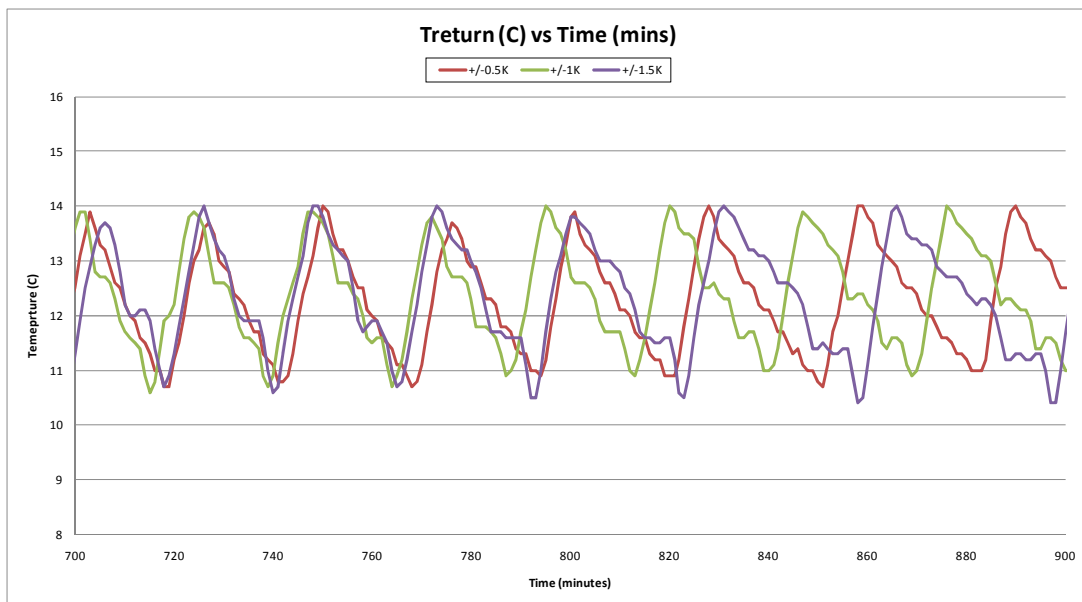


Figure 5.5 Building return temperature for different space temperatures bandwidths

T_{space} Bandwidth	± 0.5	± 1.0	± 1.5
Compressor On (%)	39.49	39.97	40.74
Compressor Off (%)	60.51	60.03	59.26
Energy Consumption - HP (kWh)	28.40	28.72	29.15
Energy Consumption - System (kWh)	57.88	58.40	59.09
Daily SPF of the HP	4.98	4.99	5.01
Daily SPF of the system	2.44	2.45	2.47

Table 5.2 System performance parameters as a function of return water bandwidth

5.4 Time Integrated Analysis

In order to characterise the accumulated system performance of the heat pump or system over an extended period (e.g., 24 hours), a number of parameters can be calculated.

5.4.1 ON/OFF Period / Cycle time

ON/OFF time operation of the heat pump can be determined, as shown in Figure 5.6, which is shown as a percentage for the heat pump in either ON and OFF mode, in this case based on a 24 hour period.

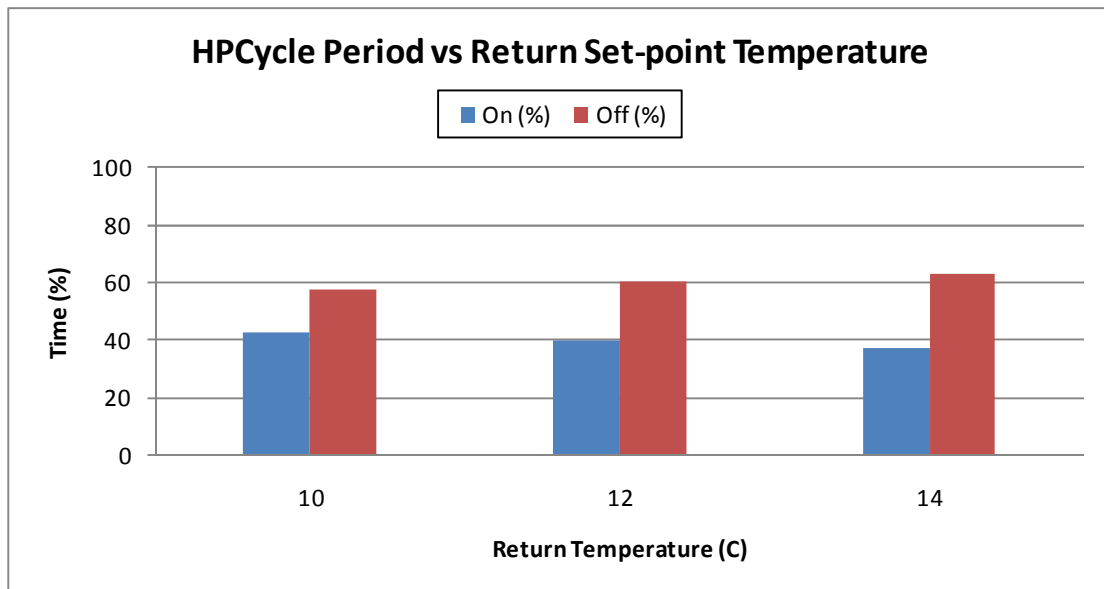


Figure 5.6 Compressor cycle period data for different water return temperatures.

5.4.2 SEASONAL PERFORMANCE FACTOR

The seasonal performance factor can be calculated with for the heat pump only and is given by Equation 17.

$$\text{SPF}_{\text{HP}} = \frac{\int_0^t \dot{Q} \cdot dt}{\int_0^t \dot{P}_{\text{HP}} \cdot dt} \quad (17)$$

If the power requirements of the secondary components (internal and external circulation pumps, fan coils) are also considered, then the seasonal performance factor from a system perspective is calculated as per Equation 18.

$$SPF_{SYSTEM} = \frac{\int_0^t \dot{Q} \cdot dt}{\int_0^t \dot{P}_{SYSTEM} \cdot dt} \tag{18}$$

Figure 5.7 illustrates, based on a 24 hour period, the total power consumed by heat pump alone (compressor) and the system power (heat pump, pumps and fan coils) as well their respective seasonal performance factors.

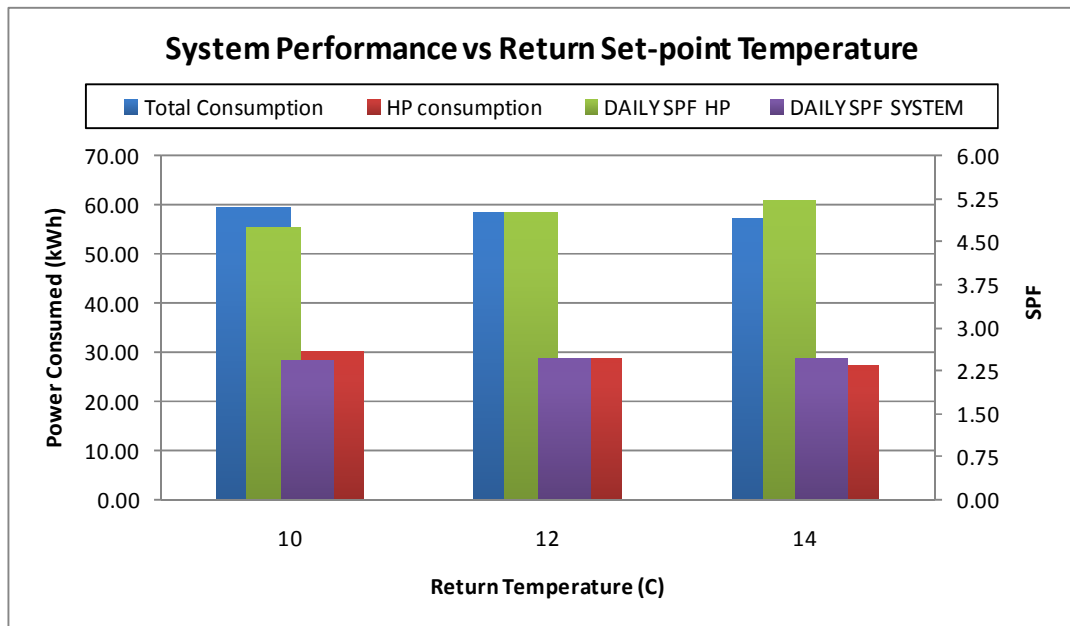


Figure 5.7 Energy consumption and daily SPF versus building water return temperatures

6 Conclusions

A heat pump system simulation model has been created using independent models of each system component that are ultimately integrated in the overall EES simulation code. Using manufacturer's data specification sheets for each component the steady-state performance of the heat pump was simulated using IMST-ART. Regression curve fit methods were used to fit correlations to the data to describe the performance of the heat pump. Models were also created for the secondary circuits components using analytic equations and correlations fit from experimental or manufacture information. The heat pump system component models were utilised in EES to simulate the steady state and quasi-steady state performance of the system. The analysis was performed to observe the effect of varying the internal and external pump frequencies on the heating capacity. The methodology for analysis of steady state, quasi-steady state, and seasonal performance are given in order to demonstrate the capabilities of the simulation model.

References

- Albieri, M. et al., (2008), 'Advanced control systems for single compressor chiller units', *International Journal of Refrigeration*, doi:10.1016/j.ijrefrig.2008.10.005.
- Braun, J. (2007), 'A Near-Optimal Control Strategy for Cool Storage Systems with Dynamic Electric Rates' *HVAC&R RESEARCH*, 13(4), 557-580
- Apra, C, Mastrullo, R, Renno, C & Vanoli, G.P. (2004), 'An evaluation of R22 substitutes performances regulating continuously the compressor refrigeration capacity', *Applied Thermal Engineering*, vol. 24 (1), 127-139.
- ASHRAE Fundamentals Handbook – SI Edition 2005, Atlanta: American Society of Heating, Refrigerating and Air-Conditioning Engineers. ISBN 4046368400.
- Chen, W, Li, Z, Deng, S. (2004), 'Capacity control of a DX VAV system and its modelling', *International Refrigeration and Air Conditioning Conference*, Purdue, July 12-15, 1-8.
- Chen, Y. (2000), 'Real-time predictive supervisory operation of building thermal systems with thermal mass', *Energy and Buildings*, 33, 141-150.
- Corberan, J. M. & Macia, J. G. (2002), 'IMST-ART, A Computer Code To Assist The Design Of Refrigeration And Air Conditioning Equipment', <http://www.imst-art.com>, IMST, Universidad Politecnica de Valencia, Spain.
- Cuevas, C, Lebrun, J. (2009), 'Testing and modelling of a variable speed scroll compressor', *Applied Thermal Engineering*, 29, 469–478.
- Cui, P, Yang, H, Spitler, J, Fang, Z (2008), 'Simulation of hybrid ground-coupled heat pump with domestic hot water heating systems using HVACSIM+', *Energy and Buildings*, 40, 1731–1736.
- Esen, H, Inalli, M, Sengur, A, Esen, M.(2007), 'Performance prediction of a ground-coupled heat pump system using artificial neural networks', *Expert Systems with Applications*, 35, 1940–1948.
- Esen, H, Inalli, M. (2009), 'Modelling of a vertical ground coupled heat pump system by using artificial neural networks', *Expert Systems with Applications*, 36, 10229–10238,
- Fahlén, P. & Karlsson, F. (2005), 'Optimizing And Controlling Media Flows In Heat Pump Systems', 8th IEA Heat Pump Conference, Las Vegas, USA, 2005.
- Flach-Malaspina, N, Lebreton, J, Clodic, D. (2004), 'Performance of a new air-to-water heat pump system with controlled capacity', *International Refrigeration and Air Conditioning Conference*, Purdue, July 12-15, 1-7.

- Gamberi, M, Manzini, R, Regattieri, A (2009), 'Simulink_ simulator for building hydronic heating systems using the Newton–Raphson algorithm' *Energy and Buildings*, 41, 848–855.
- Henze, G. P, Pfafferott, J, Herkel, S, Felsmann, C (2006), 'Impact of adaptive comfort criteria and heat waves on optimal building thermal mass control' *Energy and Buildings*, 39, 221–235
- Jain, S, Bullard, C. W. (2004), 'Capacity and Efficiency in Variable Speed, Vapour Injection and Multi-Compressor Systems', ACRC TR-227, Urbana, IL, 1-51.
- Karlsson, F, Fahlen, P. (2003), 'Energy saving potential of capacity controlled brine to-water heat pumps', *International Congress of Refrigeration*, Washington, D.C, August 17-22, 1-8.
- Karlsson, F, Fahlen, P. (2007), 'Capacity-controlled ground source heat pumps in hydronic heating systems', *Building Services Engineering*, 30(2), 221-229.
- Krause, P. E and Bullard C. W. (1994), 'Cycling and Quasi-Steady Behavior of a Refrigerator', ACRC TR-58, Urbana, IL, 1-79.
- Lax, P. D. & Wendroff, B. (1960), 'System Of Conservation Laws', *Commun. Pure Applied Mathematics* 13: pp. 217-237.
- Lindholm, T, Hoflund, R, Zhou, Y.(2005), 'Design and optimum control of a Swedish dualsource (air and ground) heat pump system' Department of Energy and Environment/Building Services Engineering, Chalmers University of Technology, Gothenburg, Sweden
- Ma, Z, Wang, S. (2009), 'An optimal control strategy for complex building central chilled water systems for practical and real-time application', *Building and Environment*, 44, 1188-1198.
- Qureshi, T. Q, Tassou S.A. (1995), 'Variable-speed capacity control in refrigeration systems', *Applied Thermal Engineering*, 16 (2), 103-113.
- Riviere, P, Malaspina, F, Lebreton, J. (2004) 'A new installation for part load testing of air to water single stage chillers and heat pumps', *International Refrigeration and Air Conditioning Conference*, Purdue, July 12-15, 1-8.
- Sakellari, D. M, Forsen, M, Lundqvist, P. (2006), 'Investigating control strategies for a domestic low-temperature heat pump heating system', *International Journal of Refrigeration*, 29, 547–555.
- Shao, S, Shi, W, Li, X, Chen, H. (2004), 'Performance representation of variable-speed compressor for inverter air conditioners based on experimental data', *International Journal of Refrigeration*, 27, 805–815.
- Shimma, Y, Tateuchi, T, Sugiura, H. (1988), 'Inverter control systems in a residential heat-pump air-conditioner' *ASHRAE Trans*, Paper HI-85-31(2), 1541-1552.

Spindler, H ,Norford, L. (2008), ‘Naturally ventilated and mixed-mode buildings Part I: Thermal modeling’ *Building and Environment*, 44, 736–749.

Spindler, H ,Norford, L. (2008), ‘Naturally ventilated and mixed-mode buildings Part II: Optimal control’, *Building and Environment*, 44, 750–761.

Sreedharan, P., ‘Evaluation of chiller modelling approaches and their usability for fault detection’, Thesis, University of California, Berkeley, USA, 2001

Vargas, J.V.C, Parise, J.A.R. (1994), ‘Simulation in transient regime of a heat pump with closed-loop and on-off control’, *International Journal of Refrigeration*, 18 (4), 235-243.

Wang, S. K, Lavan, Z. (1999), ‘Air conditioning and refrigeration engineering Air conditioning and refrigeration engineering’, ISBN 0849300576, 9780849300578 CRC Press, Pg.116.

Yang , H, Cui, P, Fang, Z (2009), ‘Vertical-borehole ground-coupled heat pumps: A review of models and systems’ *Applied Energy*, 87, 16–27.

Yang, Z, Pedersen, G. K. M. (2007), ‘Modelling and Control of Indoor Climate Using a Heat Pump Based Floor Heating System’, The 33rd Annual Conference of the IEEE Industrial Electronics Society (IECON) Nov. 5-8, Taipei, Taiwan, 1-6

Yu, F.W, Chan, K.T. (2008), ‘Environmental performance and economic analysis of all-variable speed chiller systems with load-based speed control’, *Applied Thermal Engineering*, 29, 1721–1729.

Zaheer-uddin, M, Zheng, R. (1999), ‘Optimal control of time-scheduled heating, ventilating and air conditioning processes in buildings’ *Energy Conversion & Management*, 41, 49-60.